The Positive Transcriptional Elongation Factor (P-TEFb) is required for Neural Crest Specification

Victoria L. Hatch, Marta Marin-Barba, Simon Moxon[1], Christopher T. Ford, Nicole J. Ward, Matthew L. Tomlinson, Ines Desanlis, Adam E. Hendry, Saartje Hontelez[2], Ila van Kruijsbergen[2], Gert Jan Veenstra[2], Andrea E. Münsterberg and Grant N. Wheeler[3]

School of Biological Sciences, University of East Anglia, Norwich Research Park, Norwich, NR4 7TJ, UK.

[1] present address The Genome Analysis Centre (TGAC), Norwich Research Park, Norwich, NR4 7UH, UK

[2] Radboud University, Department of Molecular Developmental Biology, Faculty of Science, Radboud Institute for Molecular Life Sciences, Nijmegen, NL

[3]Author for correspondence:

e-mail: grant.wheeler@uea.ac.uk

Tel: 44 (0)1603 593988

Fax: 44 (0)1603 592250

Key words: Neural crest cells, leflunomide, transcriptional elongation, *c-Myc*, P-TEFb, Xenopus, polymerase pausing, Cdk9, CyclinT1

Abstract

Regulation of gene expression at the level of transcriptional elongation has been shown to be important in stem cells and tumour cells, but its role in the whole animal is only now being fully explored. Neural crest cells (NCCs) are a multipotent population of cells that migrate during early development from the dorsal neural tube throughout the embryo where they differentiate into a variety of cell types including pigment cells, cranio-facial skeleton and sensory neurons. Specification of NCCs is both spatially and temporally regulated during embryonic development. Here we show that components of the transcriptional elongation regulatory machinery, CDK9 and CYCLINT1 of the P-TEFb complex, are required to regulate neural crest specification. In particular, we show that expression of the proto-oncogene *c-Myc* and *c-Myc* responsive genes are affected. Our data suggest that P-TEFb is crucial to drive expression of *c-Myc,* which acts as a 'gate-keeper' for the correct temporal and spatial development of the neural crest.

Introduction

RNA polymerase pausing and transcriptional elongation is important in the specification of many types of cells including embryonic stem (ES) cells. In order for genes to undergo transcription, RNA polymerase II (Pol II) must be recruited to the promoter region (Hochheimer and Tjian, 2003). Subsequent to this, RNA Pol II may undergo regulation to temporally control the expression of genes in specific cell types. Such regulation includes the promoter proximal pausing of Pol II, the process by which Pol II undergoes stalling or poising at the 5' end of a gene just downstream of the transcription start site (Core and Lis, 2008). This occurs due to binding of pause factors, DRB-sensitivity inducing factor (DSIF), negative elongation factor (NELF) and Gdown1 (Cheng et al., 2012; Wada et al., 1998; Yamaguchi et al., 1999). In order for transcriptional elongation to commence the positive transcription elongation factor (P-TEFb) must be recruited to the transcription elongation complex. P-TEFb is known to be a complex composed of cyclin dependent kinase 9 (CDK9) and cyclin T1 (Bres et al., 2008; Fujita et al., 2009; Jonkers and Lis, 2015; Kohoutek, 2009). To initiate transcriptional elongation, P-TEFb phosphorylates serine2 of the c-terminal domain (CTD) of Pol II and the SPT5 subunit of DSIF. After this phosphorylation, NELF dissociates from the complex and transcriptional elongation begins (Fujita et al., 2009). This process occurs when P-TEFb is in its active form and part of a collective of several proteins, termed the super elongation complex (SEC), which is known to regulate transcriptional elongation (Luo et al., 2012a; Zhou et al., 2012).

The SEC is recruited to the promoter region of genes when rapid transcription is required in response to specific developmental signals, changes to available nutrition or even acute temperature change. It is because of this that the genes primarily regulated by RNA polymerase pausing are master regulator genes and/or rapid response genes such as heat shock and serum inducible genes (Fuda et al., 2009; Luo et al., 2012b). It has also been suggested that the main function of SEC recruitment to paused genes is not necessarily to allow rapid induction but also to synchronise genes in development (Boettiger and Levine, 2009). Work in *Drosophila* and ES cells has shown that transcription elongation is not important globally within the genome but is found to regulate 10-40% of genes. Some of these genes have been identified as crucial developmental control genes (Gaertner and Zeitlinger, 2014; Zeitlinger et al., 2007).

The neural crest is a transient embryonic cell population found exclusively in vertebrates. Neural crest cells (NCCs) migrate from the dorsal neural tube to various parts of the embryo where they differentiate to give rise to a diverse set of cell types (Milet and Monsoro-Burq, 2012; Pegoraro and Monsoro-Burq, 2013; Sauka-Spengler and Bronner-Fraser, 2008). These include enteric ganglia, neuroendocrine cells, melanophores, and craniofacial skeletal and connective tissue, thus NCCs are multi-potent progenitors. Their induction and specification begins during the early gastrula stage of development and continues throughout organogenesis. This process depends on multi-module gene regulatory networks acting between the neural plate, non-neural ectoderm and paraxial mesoderm (Buitrago-Delgado et al., 2015; Hoppler and Wheeler, 2015; Huang and Saint-Jeannet, 2004; Sauka-Spengler

and Bronner-Fraser, 2008). Multiple signals and transcription factors are responsible for neural crest (NC) properties such as multipotency, induction, specification, migration and differentiation (Sauka-Spengler and Bronner-Fraser, 2008).

Once the neural plate border is fully specified and NCCs have been induced, neural crest specifiers begin to act (Milet and Monsoro-Burq, 2012). These include the transcription factors *Snail1*, *Snail2* (*Slug*), *Sox8*, *Sox9*, *Sox10*, *FoxD3*, and *c-Myc*. After specification morphological changes in the neural crest cells including changes to shape, adhesion and cell motility enable the cells to migrate from the dorsal neural tube (Sauka-Spengler and Bronner-Fraser, 2008). Neural crest specifiers can be separated into two groups; early and late NC specifiers. Expression of early neural crest specifiers, including *c-Myc*, and *Snail1*, is first identified at the neural plate border, whilst expression of slightly later neural crest specifiers such as *Snail2* and *FoxD3* is seen in pre-migrating neural crest and can continue throughout migration. Only after these have all started to be expressed does expression of members of the SoxE family such as *Sox10* start (Sauka-Spengler et al., 2007). It has been suggested that the early neural crest specifier *c-Myc* may have a role in maintaining neural crest cell multipotency and proliferation by maintaining a balance between cell death and proliferation following NC specification (Bellmeyer et al., 2003; Kee and Bronner-Fraser, 2005; Light et al., 2005).

Using chemical genetic screens we have previously identified small molecules that affect pigment cell development (Tomlinson et al., 2005; Tomlinson et al., 2009a; Tomlinson et al., 2009b). One of these, the small molecule leflunomide, inhibits pigment cell development in *Xenopus* and

Zebrafish (Elworthy et al., 2003; Tomlinson et al., 2009b; White et al., 2011). In addition, leflunomide inhibits melanoma tumour growth in tissue culture and in mouse xenografts. Leflunomide inhibits the enzyme dihydro-orotate dehydrogenase, a rate limiting enzyme in the pyrimidine biosynthesis pathway. It acts to inhibit transcriptional elongation of genes required for neural crest development and melanoma growth by limiting the pool of pyrimidines in the cell (White et al., 2011).

Here we further investigate leflunomide's ability to inhibit transcriptional elongation during neural crest development and show that it prevents expression of both, early and late neural crest specifiers such as *Snail2*, *Sox10* and *FoxD3* and *c-Myc*. As leflunomide acts through inhibiting transcriptional elongation we speculated that regulation of transcriptional elongation could be crucial for neural crest development. We therefore characterised the temporal and spatial expression of components of the Positive Transcription Elongation Factor B (P-TEFb) complex, *Cdk9* and *CyclinT1*, during neural crest development in *X. laevis*. CDK9 and CYCLINT1 loss-of-function analyses by morpholino knockdown closely mimic the phenotypes induced by leflunomide treatment. Interestingly, we identify *c-Myc* as a gene susceptible to regulation of transcriptional elongation in the early NC and show that it is able to rescue CDK9 and CYCLINT1 morphant phenotypes. This is backed up by ChIP sequencing data of *Xenopus* embryos which shows the *c-Myc* gene to be one of the most 'paused' genes in the genome. We thus propose regulation at the level of transcriptional elongation to be important in NC development through the driving of *c-Myc* expression.

Results

The expression of the P-TEFb complex components during Xenopus laevis development

We have previously shown that inhibition of transcriptional elongation leads to defects in neural crest development (White et al. 2011). An important regulator of transcriptional elongation is the P-TEFb complex. We therefore decided to investigate the role of the components of the P-TEFb complex during *Xenopus* development. The P-TEFb complex is comprised of CDK9 and CYCLINT1. Expression analysis showed *Cdk9.S*, *Cdk9.L and CyclinT1* to be expressed in the neural plate and neural plate border of neurula stage embryos (**Fig. 1**). In tailbud stage embryos at stages 26 and 32 expression was seen in the NC derived branchial arches. To determine if their expression overlapped with the NC, we carried out double *in situ* hybridisations at st16 for all three P-TEFb components with the neural crest marker Sox10. Expression of the *Cdk9.S*, *Cdk9.L* and *CyclinT1* overlapped with expression of *Sox10*, indicating that the P-TEFb complex is expressed in neural crest cells (**Fig. 1)**.

Leflunomide treatment affects the development of neural crest derivatives

Leflunomide was identified as an inhibitor of NC as a result of chemical screens carried out with the aim to look for small molecules that affect pigment cell development. Our previous results concentrated on the effects of leflunomide on zebrafish neural crest (White et al., 2011). Here we look at the effects of leflunomide in more detail on *Xenopus* neural crest. Leflunomide inhibits the formation of *Xenopus laevis* melanophores in a dose dependent manner and causes a loss of melanophores when added to the embryo after

gastrulation (**Fig. 2A and B**). Initially, a leflunomide dose response was used to establish the general phenotype induced by the compound. DMSO treated embryos served as a control. Embryos were treated at a range of concentrations from stage 15 and analysed at stage 38 (**Fig. 2Ai**). Leflunomide treatment led to a loss of melanocytes in the underside of the tail, head and lateral stripe of the embryo (**Fig. 2Ai** black arrow heads). This phenotype was dose dependant, with 60 μM leflunomide demonstrating the most severe phenotypes occurring in a significant number of embryos (**Fig. 2Bi**). Treating *Xenopus* embryos at earlier stages showed a stronger effect on pigment cell development along with a shortened axis (**Fig. 2Aii and Bii**).

Leflunomide inhibits transcription of neural crest specifier genes.

Next, we looked at how leflunomide treatment affects the expression of genes known to play a role at different stages of neural crest development. Embryos were treated with 60 μM leflunomide or DMSO from fertilisation and examined by *in situ* hybridisation for different markers of neural crest development (**Fig. 2C and D**). The expression of the neural plate border markers *Zic1*, *Zic3* and *Pax3* did not change after leflunomide treatment when compared to the DMSO control (**Fig. 2C**). This suggests that leflunomide does not interfere with these early stages of neural crest development. There was also no significant change seen in *Sox2* expression throughout the neural plate (**Fig. 2C**) suggesting that neural development is largely unaffected by leflunomide treatment. We next tested genes known to play a role in neural crest specification. The earliest neural crest specifier gene, which showed a loss in expression was *c-Myc*. This gene gave an interesting expression pattern

as it appeared that leflunomide-mediated inhibition of *c-Myc* expression was restricted to the areas fated to become neural crest (**Fig. 2D** black arrows). Loss of *c-Myc* expression was not observed in more posterior neural domains. Later neural crest specifiers, such as *Sox10*, were also significantly reduced after leflunomide treatment (**Fig. 2D** black arrows) and also shown to be only affected in the NC as expression in the otic vesicle (ear) was not affected (**Fig. S8**). In addition we examined the neural crest specifiers Slug/*Snail2* and *FoxD3* (**Fig. 2D**). Many embryos showed a partial loss or an alteration in the expression of these genes. Quantification of these results (**Fig. S1 A**) showed that *c-Myc* and *Sox10* show the strongest loss of expression. These results were confirmed by qRT-PCR on whole embryos (**Fig. S1 B**). Using this technique we found that neural plate border markers *Zic1*, *Zic3*, *Pax3* and the neural plate marker *Sox2* displayed no significant change in expression level (**Fig. S1 B**). Similarly to the *in situ* hybridisation data we saw a significant decrease in expression of neural crest specifying genes *c-Myc*, *Sox10*, *Slug/Snail2*, and *Sox9* (**Fig. S1 B**).

RNA sequencing carried out on animal caps treated with leflunomide

To characterise the tissue specific effects of leflunomide treatment we carried out RNA sequencing on animal cap explants induced to become neural crest, neuroectoderm or ectoderm. Animal caps were cut at stage 9 and immediately immersed into either 60 μM leflunomide or DMSO and allowed to develop until stage 15. The genes predominantly down-regulated in the neural crest animal cap sample were genes involved in neural crest specification and general development (**Fig. 2E** and **Fig. S1 C**). Most of these genes, were

previously identified to be affected by *in situ* hybridisation such as *c-Myc*, *Sox10*, *FoxD3*, Slug/*Snail2* and *Sox9*. Interestingly Snail1 expression was not affected by leflunomide. In agreement with our *in situ* data, we saw no change in neural plate markers, such as *Sox1* and *Sox2*, or neural plate border markers, such as *Zic1*, *Zic3* and *Pax3*. Other categories of down regulated genes included genes involved in eye development and metabolism, both of which are closely associated with neural crest development. Interestingly we saw down-regulation of heat shock genes (*Hsp90aa1.1*, *Hsp105* and *Hsp110*), which were some of the first genes suggested to be controlled by RNA polymerase pausing and transcriptional elongation (Andrulis et al., 2000; Keegan et al., 2002; Lis et al., 2000). The neuroectoderm sample showed a decrease in the expression of genes, which restrict neuroectoderm fate e.g. Grainyhead-like 3, suggesting an increase in neuroectoderm cell fate. The ectoderm sample showed no significant increase or decrease in any other genes suggesting that regulation of transcriptional elongation is not important for ectoderm development. These results indicate that interference with transcriptional elongation in this system mostly affects neural crest development. We found expression of *c-Myc* to be slightly downregulated in the neural crest sample with no change seen in the neuroectodem sample and it only shows low expression in the ectoderm. This result agrees with the *in situ* hybridisation results obtained (**Fig. 2D**). The small decrease in the NC sample is likely due to a masking of any decrease by contaminating neural tissue, which is always found in the NC animal caps. A full list of all genes affected in all three sample types can be found in **Supplementary data 1**. Overall, this data confirmed our findings that

leflunomide acts to inhibit NC development and that this could be due to inhibition of transcriptional elongation.

Knockdown of the P-TEFb components leads to defects in neural crest development

To determine the requirement of the P-TEFb complex and subsequent transcriptional elongation for NCC development, we carried out knockdown studies of the individual components. We obtained morpholinos (MO) for CDK9.S, CDK9.L and CYCLINT1. Morpholino sequences and controls are shown in **Fig. S2**. CDK9 MOs were injected individually and in combination at the one or two cell stage. Embryos injected with these morpholinos were left to develop until stage 38. The phenotype obtained after knockdown of the P-TEFb components was comparable to that obtained after leflunomide treatment. The MO-injected embryos displayed neural crest defects including loss of pigment cells (**Fig. 3A and Fig. S3A**) comparable to those shown in **Fig. 2** and disorganisation of cranial cartilage (**Fig S3B**).

We next carried out *in situ* hybridisation using neural plate border genes, neural crest specifier genes and a neural plate marker. Embryos were injected with a standard control Morpholino, CDK9.S morpholino or the CYCLINT1 morpholino along with 300 pg of *LacZ* cRNA into one cell of a two-cell stage, with the non-injected half serving as control (**Fig. 3B Fig. S3D and Fig. S7**). The expression of neural plate border markers *Zic1*, *Zic3* and *Pax3* were not affected (**Fig. 3B**). The Neural plate marker *Sox2* and other neural genes were not affected (**Fig 3B and S5**). *c-Myc* and *Sox10* however, showed a striking knockdown after CDK9.S-MO or CYCLINT1-MO (**Fig. 3B**). Loss of *c-Myc* was

seen specifically in the anterior patches, which give rise to NC (black arrows **Fig. 3B**). Complete loss of *Sox10* expression was seen in the NC (black arrows **Fig. 3B**). These results were confirmed using qRT-PCR (**Fig. S4C**). The same experiment was carried out after injection of the CDK9.L MO, or a combination of the CDK9.S and CDK9.L MOs and this data is shown in **Fig. S4A and B**. When embryos were allowed to progress to stage 26 an effect on Sox10 expression in the cranial NC can be seen but no change in expression of Sox10 is seen in the otic vesicle (**Fig. S8**). In Leflunomide treated embryos Sox10 expression in the otic vesicle is also not affected while there is a loss of expression in the cranial NC and pigment cells (**Fig. S8**). Other neural crest markers Slug/*Snail2*, *FoxD3* and *Sox9* show some alteration and partial loss of expression, but very little complete loss of expression (**Fig. 3B and Fig. S4**)**.** In support of the RNA-Seq data expression of Snail1, which is also an early specifier of NC, was not affected by knockdown of P-TEFb components (**Fig. S7**). The phenotypes after P-TEFb knock-down were strikingly similar to those obtained after leflunomide treatment (**Figs. 2C and D**).

c-Myc is also known to regulate the development of trigeminal placodes in the anterior region of the embryo. We therefore looked at the expression of placodal markers by WISH. The placode markers we used include *Tbx2*, *NeuroD* and *ElrD*, which are expressed in the trigeminal placodes and the neural tube (Green and Vetter, 2011; Schlosser and Ahrens, 2004; Showell et al., 2006). We were able to detect a loss of expression of all three markers, specifically in the trigeminal placode region, but not in any of the other tissues in which they are expressed (**Fig. 3C and Fig. S4D**).

c-Myc is a paused gene during development

As *c-Myc* is the earliest gene to be affected by Leflunomide and the knockdown of the P-TEFb components, we looked at the RNA pol II occupancy profile of *c-Myc* and compared it to the promoter histone modification H3K4me3 and the processive elongation mark H3K36me3. These data suggest that *c-Myc* is in a paused or poised state during mid to late gastrula just before the NC are specified (**Fig. 4A**). We next carried out RNA Pol II ChIP-seq on embryos injected with CDK9.S morpholino compared to embryos injected with control morpholino. Knockdown of Cdk9 causes an increase in RNA Pol II occupance, the effect of which is the stongest on the promoter, suggesting that there is an increase in pausing of *c-Myc* (**Fig 4A**, blue tracks). We determined the pausing index values for all annotated genes and **Fig 4Bi** shows that there is an overall increase in pausing. This would be expected given that transcriptional elongation is effectively being suppressed. **Fig 4Bii** highlights that the loss of CDK9 causes an increase in the amount of RNA Pol II bound to the promoter compared to the rest of the gene body. The position of c-Myc is shown by the blue spot. While the RPKM on its gene body is increased from 5 to 10, the RPKM on its TSS goes from 11 to 50. This suggests that c-Myc is particularly sensitive to control of expression at the level of transcriptional elongation and is therefore in a more 'paused' state.

c-Myc is regulated by transcriptional elongation in neural crest cells

We postulated that *c-Myc* could be the primary gene regulated by transcriptional elongation in neural crest cells. We therefore examined if loss of *Sox10* expression after P-TEFb morpholino injection could be rescued by co-

injecting *c-Myc* RNA. For this experiment CDK9.S morpholino and CYCLINT1 morpholinos were injected alone or with 100 pg of *c-Myc* and 500pg of *c-Myc* RNA. As before, knockdown of CDK9.S and CYCLINT1 led to a high number of embryos displaying loss of *Sox10* expression (**Fig. 5A and B**). Co-injection of these morpholinos with 100 pg of *c-Myc* resulted in a reduction of the number of embryos displaying a loss of expression phenotype. The majority of embryos displayed a partial loss phenotype or wild type phenotype. After injection of 500 pg of *c-Myc* RNA a greater number of embryos displayed a wild type phenotype (**Fig. 5A and B**). Injection of 500 pg of *c-Myc* alone had very little effect on *Sox10* expression and injection of the standard control MO did not affect *Sox10* expression (**Fig. 5B**). Injection of c-Myc RNA into one blastomere was also shown to rescue leflunomide treated embryos on the injected side (**Fig S6**).

Discussion

The molecular mechanisms controlling NCC specification and differentiation are complex and consist of many layers of regulation to ensure the cells decide upon the correct lineage and form the correct cell types. Other multipotent cell types such as embryonic stem cells and haematopoietic stem cells are thought to undergo regulation at the level of transcriptional elongation (Bai et al., 2010; Lin et al., 2011). It has previously been shown that *Foggy* mutant Zebrafish, which are deficient in the SPT5 subunit of DSIF, display pigmentation and cardiac defects suggesting a disruption in neural crest development (Keegan et al., 2002). In addition the *Xenopus tropicalis* mutant cyd vicious, which displays pigmentation defects, is also mutated in the *Spt5* gene (Lyle Zimmerman, personal communication). Here we provide evidence for direct regulation of the specification of NC at the level of transcriptional elongation by the P-TEFb complex. In addition, we show that in the NC, *c-Myc* is the crucial gene regulated at the level of transcriptional elongation.

The methods used in this study were firstly to use leflunomide as an inhibitor of transcriptional elongation and secondly, through the use of morpholino knockdowns of components of the P-TEFb complex to block transcriptional elongation. Both of these methods gave comparable results (**Figs. 2 and 3, Figs S1-4**). Both demonstrate a disruption in the development of neural crest derivatives including melanophores, sensory neurons and cranio-facial cartilage. When looking at the levels of expression of genes involved in the neural crest gene regulatory network the two genes demonstrating the greatest level of knockdown by WISH*,* qRT-PCR or RNAseq were *c-Myc,* an early NC specifier and *Sox10,* a NC specifier downstream of *c-Myc* also expressed in the migrating NC. Furthermore, we showed that the loss

of *Sox10* gene expression in the NC was rescued by injecting embryos with *c-Myc* RNA (**Fig. 5**).

To investigate whether *c-Myc* expression was directly regulated by the P-TEFb complex and transcriptional elongation, we looked at cell types other than neural crest cells, which are known to have *c-Myc* within their gene regulatory network. We reasoned that if *c-Myc* is a direct target a loss in expression of markers for these other cell types should be observed. Our *in situ* hybridisation data suggested that *c-Myc* expression in the placodal regions is lost after knockdown of P-TEFb components (**Fig. 3B**), as opposed to more posterior neural expression, which was not affected. We therefore looked at the trigeminal placodes, which are similar to NC and which express *c-Myc* in the early stages of their gene regulatory network (Bellmeyer et al., 2003; Grocott et al., 2012). We were able to detect a loss of expression of three markers, specifically in the trigeminal placode region, but not in any of the other tissues in which they are expressed (**Fig. 3C and Fig. S4D**). This provides further evidence for *c-Myc* itself being directly regulated by transcriptional elongation in specific tissues. Interestingly we also see a loss of Rohon-Beard cell markers (Runx1, Islet1 and Ngnr1) upon knockdown of the P-TEFb complex (**Fig S4E**). It is currently not known whether c-Myc signalling is required for the development of these cells. The combination of the loss of neural crest cells, trigeminal placodes and Rohon-Beard cells causes embryos treated with leflunomide or CDK9 morpholino to become insensitive to touch response assays as shown in (**Fig S3C and Supp movies 1-3**).

Our ChIP-Seq analysis (**Fig 4**) shows c-Myc to be a paused gene during early development and that the inhibition of transcriptional elongation by Cdk9

morpholino causes *c-Myc* to become even more paused compared to the rest of the genome. This is consistent with studies using human 293T embryonic kidney cell lines, which have also shown *c-Myc* to be a paused gene (Takahashi et al., 2011). Rahl and colleagues (Rahl et al., 2010) have previously shown in tissue culture that c-MYC can directly regulate the activity of P-TEFb. This suggests the activation of *c-Myc* by signals such as WNT (Bellmeyer et al., 2003) could lead to a positive feedback system where c-MYC activates P-TEFb which in turn promotes transcriptional elongation of the *c-Myc* gene. Our rescue experiments in **Fig 5** and **Fig S6** suggests c-Myc overexpression can overcome the effect of loss of P-TEFb activity. However we cannot exclude the possibility that the increased amount of c-MYC in these embryos may increase any residual P-TEFb activity to overcome the loss of activity from the MO. Either way it still underlines the crucial role for regulation at the level of transcriptional elongation and the role of *c-Myc* in this process.

Our RNA-Seq results using animal cap explants show that when the three cell types NC, neuroectoderm and ectoderm have inhibited transcriptional elongation the only cell type to show specific changes was the NC. We show down regulation of *c-Myc* expression in the neural crest sample and observed little change in the neural and ectoderm samples (**Supplementary data 1**). This gives us further reason to suggest that regulation of *c-Myc* expression by transcriptional elongation is occurring only in specific tissues, in this case the NC.

Overall, these results provide evidence that *c-Myc* is the ‘gate-keeper’ regulated by transcriptional elongation in both, the NC and trigeminal placodes, and that expression of the downstream marker *Sox10* in the NC is lost as a

secondary effect of this. This is consistent with previous analysis of microarrays from melanoma tumours where many *c-Myc* responsive genes were affected by leflunomide treatment (White et al., 2011). Our results are summarised as a model in **Fig. 6**. We propose that the *c-Myc* gene is held in a paused state within NCCs and not in all tissues. This paused state is then specifically released in a wild type NC cell by the P-TEFb complex to allow normal *c-Myc* transcription and therefore promote synchronous transcription of downstream genes such as *Sox10* and the subsequent differentiation of neural crest derivatives (**Fig. 6** top route). MYC is known to actually stimulate recruitment of P-TEFb to promoters of active genes thus leading to increased expression in a process called transcriptional amplification (Rahl and Young, 2014). The results obtained from our P-TEFb knockdown studies and leflunomide treated embryos suggest that when the function of P-TEFb is impaired *c-Myc* is no longer expressed at a high enough level and this in turn leads to incorrect expression of downstream NC specifiers such as *Sox10* and the synchronicity of maintaining multipotency, proliferation and differentiation of neural crest is lost (**Fig. 6** bottom route). Recently it has been shown that regulation of transcriptional elongation to be important for genes regulating cell cycle and signal transduction (Williams et al., 2015). *c-Myc* is an important regulator for such processes and as we show here it is clearly important in the regulation of the neural crest.

To conclude, we provide evidence that the P-TEFb activation of transcriptional elongation is an important step regulating the correct expression of neural crest genes and that this is mediated through the action of *c-Myc*. It is possible that a polymerase pausing step is acting to prime *c-Myc* for

transcription to ensure the correct temporal expression of NC genes and therefore a synchronous development of this cell type into its derivatives. Polymerase pausing has previously been shown to be important in cells, which undergo synchronous gene expression and development. Compared to stochastic uncoordinated gene expression in the whole embryo, the development of the NC requires such synchronous gene expression (Boettiger and Levine, 2009). *c-Myc* has been shown here to be particularly sensitive to inhibition of transcriptional elongation and so it is possible that *c-Myc* is a paused gene in prospective NC cells (Bai et al., 2010). There has been much debate in recent literature as to whether this phenomenon of RNA polymerase pausing and regulation of transcriptional elongation is (1) common to all genes and (2) whether it might be specific to certain cell types (Luo et al., 2012b). Our data contributes to this debate by providing evidence that regulation of transcriptional elongation is focussed on c-Myc and is particularly important in developing neural crest.

Materials and Methods

Embryos, capped RNA synthesis, morpholinos, microinjection and animal capping

All experiments were performed in compliance with the relevant laws and institutional guidelines at the University of East Anglia. The research has been approved by the local ethical review committee according to UK Home Office regulations. *Xenopus laevis* embryos were obtained as previously described (Harrison et al., 2004). Embryos were staged using the Nieuwkoop and Faber normal table of *Xenopus* development (Nieuwkoop, 1994). Full length cDNAs for *Xenopus laevis CDK9.S* (IMAGE:5156812) and *CyclinT1* (IMAGE:7207389) were obtained from the IMAGE Clone collection. CDK9.L was obtained from Dr Paul Mead. The cDNA clones were all completely sequenced before subcloning into relevant vectors. Capped RNA was synthesised using the SP6 mMESSAGE mMACHINE^{TM} (Ambion) kit for *Wnt1*, *Noggin*, *c-Myc* (from Carole Labonne), *LacZ* and mutagenesis rescue constructs for *CDK9.S*, *CDK9.L* and *CyclinT1*. Mutagenesis was carried out using the QuickChange II XL Site-Directed Mutagenesis kit (Agilent Technologies). Morpholino oligos (MOs) were designed and made by Gene Tools. Morpholino sequences are: Standard control (CoMO) 5'-CCTCTTACCTCAGTTACAATTTATA-3', *CDK9.S* 5'-ATGGCCAAGAACTACGACTCGGTGG-3', *CDK9.L* 5'-ATGGTAAAGAACTACGACTCTGTTG-3'and *CyclinT1* 5'-GACATCGTACTTTATGGCAACAAAC-3'. These were tested by in vitro translation using the TNT® Coupled Reticulocyte Lysate System (Promega)

following manufacturers instructions. Capped RNA and morpholinos were co-injected with 300 pg *LacZ*. Microinjections were carried out in 3% Ficoll PM400 (Sigma). Embryos were injected at the 2 cell stage in either 1 or both cells. β-Galactosidase activity was detected by colorimetric reaction using Red-Gal (Sigma). Embryos were staged and fixed for 2 hours at room temperature in MEMFA. Animal capping was carried out as previously described (Garcia-Morales et al., 2009).

Wholemount in situ hybridisation

Single and double in situ hybridisation was carried out as previously described (Harrison et al., 2004). Probes were synthesised for *c-Myc* (IMAGE:4884683), *Sox10*, *Zic1*, *Zic3*, *Pax3*, *Sox2*, Slug/*Snail2*, *FoxD3*, *Sox9*, *CDK9.S*, *CDK9.L* and *CyclinT1*.

Cryosectioning

Embryos were fixed in MEMFA for 1 hour, washed twice for 5 minutes in PBST and then put in 30% sucrose for 4 hours at room temperature. Embryos were then transferred to cryomoulds filled with optimal cutting temperature (OCT) compound and left at 4^{o}C overnight. Embryos were then positioned appropriately for sectioning and left at -20^{o}C overnight. Embryos were sectioned using the LEICA CM 1950 Cryostat and sections were placed on 5% TESPA slides. Slides were then washed for 5 minutes in PBST and covered with a coverslip using hydromount. Images were taken using a Zeiss CCD upright microscope with colour camera.

Alcian blue staining

Embryos were fixed for 1 hour at room temperature, dehydrated with 5 washes of 100% ethanol (EtoH) for 5 minutes each at RT and then left in Alcian blue staining solution for 3 nights. After this they were washed 3 times for 15 minutes in 95% ethanol at RT then rehydrated in 2% KOH. This was done gradually using 10 minute washes of 75% EtoH in 2% KOH, 50% EtoH in 2% KOH, 25% EtoH in 2% KOH then 3 2% KOH washes. Embryos were then stored in glycerol to make embryos more transparent. Facial cartilage was then dissected out before imaging.

RNA extraction, PCR, Q-PCR and RNA sequencing

For the PCR, Q-PCR and RNA-sequencing experiments animal caps were cut at stage 8 and allowed to develop to stage 15. Approximately 200 caps were required for each condition tested to generate enough RNA for sequencing. Caps were collected in batches of approx. 30 and RNA purified. Each batch was tested by RT_PCR or QPCR to make sure the caps were expressing the relevant NC, neural or ectodermal markers. Total RNA was extracted using TRIzol® (15596-026, Life technologies, UK) and DNAse treated. Reverse transcription was performed using SuperScript® II reverse transcriptase (18064-014, Invitrogen, CA, USA), with 1 µg total RNA and random primers (C1181, Promega, Southampton, UK). Brightwhite 96 well plates (BW-FAST) and high quality optical plate seals (BW-ADVSEAL) were used (PrimerDesign Ltd, Southampton, UK). Gene-specific nucleotide sequences were detected using Precision™ FAST-LR 2x mastermix (PrimerDesign Ltd, Southampton, UK). Quantitative RT-PCR was performed in

a final volume of 20 µL using a 7500 FAST real-time PCR instrument (Roche) under the following cycling conditions: 95°C for 20 s, 40 cycles at 95°C for 3 s, 60°C for 30 s. After cycling, a melting curve was recorded between 60°C and 95°C under the following 95°C for 15 s, 60°C for 1 min, 95°C for 15 s, 60°C for 15 s with a ramp rate of 0.11°C□s^{-1}. Detection primers were designed using Primer3 software (http://biotools.umassmed.edu/bioapps/primer3_www.cgi) and custom designed by PrimerDesign Ltd, UK where indicated (Rozen and Skaletsky, 2000). Their oligonucleotide sequences are provided in **supplementary table 1**. In-house designed primers were synthesized by eurofins (Norwich, UK) and custom primers were designed by and purchased from PrimerDesign Ltd (PrimerDesign Ltd, Southampton, UK).

For the RNA seq experiments to determine whether we get a similar loss of neural crest specifying genes compared to the whole embryo data, the animal cap samples were initially tested by *in situ* hybridisation and RT-PCR. RNA sequencing was carried out to investigate which genes were affected by leflunomide across the whole genome in the three sample types.

For RNA sequencing total RNA was fragmented before undergoing cDNA library preparation. cDNA was end-repaired, A-tailed and adapter-ligated before amplification and size selection. The prepared libraries undergo quality control by running on a gel and using a bioanalyser to check library fragment size distribution before 100bp paired end sequencing over one lane of a flow cell. Samples were multiplexed 2 x 3 and ran on one lane each to yield approximately 25 million paired reads per sample. Reads were aligned to the *Xenopus laevis* transcriptome (xlaevisMRNA.fasta) downloaded from Xenbase (release 28/09/12) (Bowes et al., 2008; Langmead and Salzberg, 2012).

Mapping was carried out with bowtie2 on paired-end samples using default parameters. A custom Perl script was used to parse the bowtie results and count the number of sequences in each sample mapping to every mRNA sequence in the transcriptome file. The table of raw abundances for each mRNA was then read into R and differential expression between untreated and leflunomide treated samples was calculated using the DEseq package (Anders and Huber, 2010). Any transcript with a p-value of <= 0.05 was classed as being differentially expressed between untreated and leflunomide treated samples.

The data for quantitative RT-PCR experiments were analysed using the 7500FAST software. Measured Ct values for quantitative RT-PCR technical and biological replicates for each gene of interest were analysed using the NORMA-gene algorithm (Heckmann et al., 2011). NORMA-gene reduces systematic and artificial between-replicate bias utilising the entire data-set of the target genes being studied. NORMA-gene is applicable to small data sets greater than five genes of interest and is used as our primary analysis tool as it produces equal or better normalization compared to the delta-delta ct method. Leflunomide affects gene transcription thus impacting upon metabolic and neural crest pathways. Therefore, using reference vs. target normalisation is not appropriate to measure gene expression.

ChIP-sequencing

Morpholinos were injected at 2 cell stage embryos and incubated at 26^{o}C in 0.05x Marc's Modified Ringer's (MMR). Approximately 50 embryos per sample were fixed at stage 16 in 1% formaldehyde for 30min. Samples were then washed in 125mM glycine solution 30 minutes and then transfer gradually to

0.1X MMR. Embryos were homogenized in sonication buffer (20mM TrisHCl pH=8, 70mM KCl, 1mM EDTA, 10% glycerol, 5mM DTT, 0.125% NP40, protease inhibitors (Roche #04693132001) and stored at -80C. ChIP was prepared as previously described (Jallow et al., 2004). After sonication, chromatin samples were incubated with RNA Pol II antibody (diagenode C15200004) 1ug per 15 embryo equivalent in IP buffer overnight (50mM TrisHCl pH=8, 100mM NaCl, 2mM EDTA, 1%NP40, 1mM DTT and protease inhibitors) followed by incubation with Dynabeads Protein G for 1h. Beads where subsequently washed in ChIP 1 buffer (IP buffer + 0.1% deoxycholate), ChIP 2 buffer (ChIP 1 buffer + 400mM NaCl), ChIP 3 buffer (ChIP 1 buffer + 250mM LiCl) and TE buffer. Material was digested with proteinase K and DNA was purified using a QIAGEN kit. Q-PCR was performed pre and post library preparation for quality checking and DNA libraries were prepared using Kapa Hyper Prep kit (Kapa Biosysistem). Sequencing was done on the Illumina HiSeq2000 platform and reads were mapped to the reference *X. tropicalis* genome JGI7.1 using BWA allowing one mismatch.

Small molecule compound treatment

The small molecule compound leflunomide (Sigma) was dissolved in DMSO to make a 10 mM stock. This was then diluted directly into the embryos media 0.1xMMR. DMSO was added to the media as a control (Tomlinson et al., 2012).

Author contributions

VH, CF, NW, MT, MM, ID, SH, IK and AH performed experiments. VH, CF, SM, MT, GV, MM, AM and GW designed experiments, discussed and analysed data. GW directed the research. VH and GW wrote the manuscript.

Acknowledgements

We would like to thank members of the Münsterberg and Wheeler labs past and present for their help and support during this project. We would also like to thank Stefan Hoppler, Tim Grocott and Richard White for helpful discussions, Paul Mead for sending us his *Cdk9* plasmid and other colleagues for various plasmids. VH and GW acknowledge the help provided by the Cold Spring Harbor *Xenopus* course. This work was supported by a BBSRC grant (BB/I022252) to GW, a UEA Dean's studentship to VH, by the People Programme (Marie Curie Actions) of the European Union's Seventh Framework Programme FP7 under REA grant agreement number 607142 (DevCom) to MM and ID and by the UEA, the John Innes Centre and AstraZeneca to AH.

References

Anders, S., Huber, W., 2010. Differential expression analysis for sequence count data. Genome Biol 11, R106.

Andrulis, E.D., Guzman, E., Doring, P., Werner, J., Lis, J.T., 2000. High-resolution localization of Drosophila Spt5 and Spt6 at heat shock genes in vivo: roles in promoter proximal pausing and transcription elongation. Genes & development 14, 2635-2649.

Bai, X., Kim, J., Yang, Z., Jurynec, M.J., Akie, T.E., Lee, J., LeBlanc, J., Sessa, A., Jiang, H., DiBiase, A., Zhou, Y., Grunwald, D.J., Lin, S., Cantor, A.B., Orkin, S.H., Zon, L.I., 2010. TIF1gamma controls erythroid cell fate by regulating transcription elongation. Cell 142, 133-143.

Bellmeyer, A., Krase, J., Lindgren, J., LaBonne, C., 2003. The protooncogene c-myc is an essential regulator of neural crest formation in xenopus. Dev Cell 4, 827-839.

Boettiger, A.N., Levine, M., 2009. Synchronous and stochastic patterns of gene activation in the Drosophila embryo. Science 325, 471-473.

Bowes, J.B., Snyder, K.A., Segerdell, E., Gibb, R., Jarabek, C., Noumen, E., Pollet, N., Vize, P.D., 2008. Xenbase: a Xenopus biology and genomics resource. Nucleic Acids Res 36, D761-767.

Bres, V., Yoh, S.M., Jones, K.A., 2008. The multi-tasking P-TEFb complex. Curr Opin Cell Biol 20, 334-340.

Buitrago-Delgado, E., Nordin, K., Rao, A., Geary, L., LaBonne, C., 2015. NEURODEVELOPMENT. Shared regulatory programs suggest retention of blastula-stage potential in neural crest cells. Science 348, 1332-1335.

Cheng, B., Li, T., Rahl, P.B., Adamson, T.E., Loudas, N.B., Guo, J., Varzavand, K., Cooper, J.J., Hu, X., Gnatt, A., Young, R.A., Price, D.H., 2012. Functional association of Gdown1 with RNA polymerase II poised on human genes. Mol Cell 45, 38-50.

Core, L.J., Lis, J.T., 2008. Transcription regulation through promoter-proximal pausing of RNA polymerase II. Science 319, 1791-1792.

Elworthy, S., Lister, J.A., Carney, T.J., Raible, D.W., Kelsh, R.N., 2003. Transcriptional regulation of mitfa accounts for the sox10 requirement in zebrafish melanophore development. Development 130, 2809-2818.

Fuda, N.J., Ardehali, M.B., Lis, J.T., 2009. Defining mechanisms that regulate RNA polymerase II transcription in vivo. Nature 461, 186-192.

Fujita, T., Piuz, I., Schlegel, W., 2009. The transcription elongation factors NELF, DSIF and P-TEFb control constitutive transcription in a gene-specific manner. FEBS Lett 583, 2893-2898.

Gaertner, B., Zeitlinger, J., 2014. RNA polymerase II pausing during development. Development 141, 1179-1183.

Garcia-Morales, C., Liu, C.H., Abu-Elmagd, M., Hajihosseini, M.K., Wheeler, G.N., 2009. Frizzled-10 promotes sensory neuron development in Xenopus embryos. Developmental biology 335, 143-155.

Green, Y.S., Vetter, M.L., 2011. EBF factors drive expression of multiple classes of target genes governing neuronal development. Neural Dev 6, 19.

Grocott, T., Tambalo, M., Streit, A., 2012. The peripheral sensory nervous system in the vertebrate head: a gene regulatory perspective. Developmental biology 370, 3-23.

Harrison, M., Abu-Elmagd, M., Grocott, T., Yates, C., Gavrilovic, J., Wheeler, G.N., 2004. Matrix metalloproteinase genes in Xenopus development. Dev Dyn 231, 214-220.

Heckmann, L.H., Sorensen, P.B., Krogh, P.H., Sorensen, J.G., 2011. NORMA-Gene: a simple and robust method for qPCR normalization based on target gene data. BMC Bioinformatics 12, 250.

Hochheimer, A., Tjian, R., 2003. Diversified transcription initiation complexes expand promoter selectivity and tissue-specific gene expression. Genes Dev 17, 1309-1320.

Hontelez, S., van Kruijsbergen, I., Georgiou, G., van Heeringen, S.J., Bogdanovic, O., Lister, R., Veenstra, G.J., 2015. Embryonic transcription is controlled by maternally defined chromatin state. Nat Commun 6, 10148.

Hoppler, S., Wheeler, G.N., 2015. DEVELOPMENTAL BIOLOGY. It's about time for neural crest. Science 348, 1316-1317.

Huang, X., Saint-Jeannet, J.P., 2004. Induction of the neural crest and the opportunities of life on the edge. Dev Biol 275, 1-11.

Jallow, Z., Jacobi, U.G., Weeks, D.L., Dawid, I.B., Veenstra, G.J., 2004. Specialized and redundant roles of TBP and a vertebrate-specific TBP paralog in embryonic gene regulation in Xenopus. Proc Natl Acad Sci U S A 101, 13525-13530.

Jonkers, I., Lis, J.T., 2015. Getting up to speed with transcription elongation by RNA polymerase II. Nat Rev Mol Cell Biol 16, 167-177.

Kee, Y., Bronner-Fraser, M., 2005. To proliferate or to die: role of Id3 in cell cycle progression and survival of neural crest progenitors. Genes Dev 19, 744-755.

Keegan, B.R., Feldman, J.L., Lee, D.H., Koos, D.S., Ho, R.K., Stainier, D.Y., Yelon, D., 2002. The elongation factors Pandora/Spt6 and Foggy/Spt5 promote transcription in the zebrafish embryo. Development 129, 1623-1632.

Kohoutek, J., 2009. P-TEFb- the final frontier. Cell Div 4, 19.

Langmead, B., Salzberg, S.L., 2012. Fast gapped-read alignment with Bowtie 2. Nature methods 9, 357-359.

Light, W., Vernon, A.E., Lasorella, A., Iavarone, A., LaBonne, C., 2005. Xenopus Id3 is required downstream of Myc for the formation of multipotent neural crest progenitor cells. Development 132, 1831-1841.

Lin, C., Garrett, A.S., De Kumar, B., Smith, E.R., Gogol, M., Seidel, C., Krumlauf, R., Shilatifard, A., 2011. Dynamic transcriptional events in embryonic stem cells mediated by the super elongation complex (SEC). Genes & development 25, 1486-1498.

Lis, J.T., Mason, P., Peng, J., Price, D.H., Werner, J., 2000. P-TEFb kinase recruitment and function at heat shock loci. Genes & development 14, 792-803.

Luo, Z., Lin, C., Shilatifard, A., 2012a. The super elongation complex (SEC) family in transcriptional control. Nat Rev Mol Cell Biol 13, 543-547.

Luo, Z., Lin, C., Shilatifard, A., 2012b. The super elongation complex (SEC) family in transcriptional control. Nature reviews. Molecular cell biology 13, 543-547.

Milet, C., Monsoro-Burq, A.H., 2012. Neural crest induction at the neural plate border in vertebrates. Dev Biol 366, 22-33.

Nieuwkoop, P.F., J., 1994. Normal Table of Xenopus laevis (Daudin). Garlan Publishing, New York.

Pegoraro, C., Monsoro-Burq, A.H., 2013. Signaling and transcriptional regulation in neural crest specification and migration: lessons from xenopus embryos. Wiley interdisciplinary reviews. Developmental biology 2, 247-259.

Rahl, P.B., Lin, C.Y., Seila, A.C., Flynn, R.A., McCuine, S., Burge, C.B., Sharp, P.A., Young, R.A., 2010. c-Myc regulates transcriptional pause release. Cell 141, 432-445.

Rahl, P.B., Young, R.A., 2014. MYC and transcription elongation. Cold Spring Harb Perspect Med 4, a020990.

Rozen, S., Skaletsky, H., 2000. Primer3 on the WWW for general users and for biologist programmers. Methods Mol Biol 132, 365-386.

Sauka-Spengler, T., Bronner-Fraser, M., 2008. A gene regulatory network orchestrates neural crest formation. Nat Rev Mol Cell Biol 9, 557-568.

Sauka-Spengler, T., Meulemans, D., Jones, M., Bronner-Fraser, M., 2007. Ancient evolutionary origin of the neural crest gene regulatory network. Dev Cell 13, 405-420.

Schlosser, G., Ahrens, K., 2004. Molecular anatomy of placode development in Xenopus laevis. Developmental biology 271, 439-466.

Showell, C., Christine, K.S., Mandel, E.M., Conlon, F.L., 2006. Developmental expression patterns of Tbx1, Tbx2, Tbx5, and Tbx20 in Xenopus tropicalis. Developmental dynamics : an official publication of the American Association of Anatomists 235, 1623-1630.

Takahashi, H., Parmely, T.J., Sato, S., Tomomori-Sato, C., Banks, C.A., Kong, S.E., Szutorisz, H., Swanson, S.K., Martin-Brown, S., Washburn, M.P., Florens, L., Seidel, C.W., Lin, C., Smith, E.R., Shilatifard, A., Conaway, R.C., Conaway, J.W., 2011. Human mediator subunit MED26 functions as a docking site for transcription elongation factors. Cell 146, 92-104.

Tomlinson, M.L., Field, R.A., Wheeler, G.N., 2005. Xenopus as a model organism in developmental chemical genetic screens. Mol Biosyst 1, 223-228.

Tomlinson, M.L., Guan, P., Morris, R.J., Fidock, M.D., Rejzek, M., Garcia-Morales, C., Field, R.A., Wheeler, G.N., 2009a. A chemical genomic approach identifies matrix metalloproteinases as playing an essential and specific role in Xenopus melanophore migration. Chem Biol 16, 93-104.

Tomlinson, M.L., Hendry, A.E., Wheeler, G.N., 2012. Chemical genetics and drug discovery in Xenopus. Methods Mol Biol 917, 155-166.

Tomlinson, M.L., Rejzek, M., Fidock, M., Field, R.A., Wheeler, G.N., 2009b. Chemical genomics identifies compounds affecting Xenopus laevis pigment cell development. Mol Biosyst 5, 376-384.

Wada, T., Takagi, T., Yamaguchi, Y., Ferdous, A., Imai, T., Hirose, S., Sugimoto, S., Yano, K., Hartzog, G.A., Winston, F., Buratowski, S., Handa, H., 1998. DSIF, a novel transcription elongation factor that regulates RNA polymerase II processivity, is composed of human Spt4 and Spt5 homologs. Genes Dev 12, 343-356.

White, R.M., Cech, J., Ratanasirintrawoot, S., Lin, C.Y., Rahl, P.B., Burke, C.J., Langdon, E., Tomlinson, M.L., Mosher, J., Kaufman, C., Chen, F., Long, H.K., Kramer, M., Datta, S., Neuberg, D., Granter, S., Young, R.A., Morrison, S., Wheeler, G.N., Zon, L.I., 2011. DHODH modulates transcriptional elongation in the neural crest and melanoma. Nature 471, 518-522.

Williams, L.H., Fromm, G., Gokey, N.G., Henriques, T., Muse, G.W., Burkholder, A., Fargo, D.C., Hu, G., Adelman, K., 2015. Pausing of RNA polymerase II regulates mammalian developmental potential through control of signaling networks. Mol Cell 58, 311-322.

Yamaguchi, Y., Takagi, T., Wada, T., Yano, K., Furuya, A., Sugimoto, S., Hasegawa, J., Handa, H., 1999. NELF, a multisubunit complex containing RD, cooperates with DSIF to repress RNA polymerase II elongation. Cell 97, 41-51.

Zeitlinger, J., Stark, A., Kellis, M., Hong, J.W., Nechaev, S., Adelman, K., Levine, M., Young, R.A., 2007. RNA polymerase stalling at developmental control genes in the Drosophila melanogaster embryo. Nat Genet 39, 1512-1516.

Zhou, Q., Li, T., Price, D.H., 2012. RNA polymerase II elongation control. Annu Rev Biochem 81, 119-143.

Figure Legends

Figure 1: The expression of the P-TEFb complex components during *Xenopus laevis* development. Transcripts for the P-TEFb components were detected using NBT/BCIP and expression of *CDK9.S*, *CDK9.L* and *CyclinT1* appeared blue in the sectioned neurula stage embryo. *Sox10* was detected using fast red and fluorescence microscopy. (A) *CDK9.S* expression at stage 16 and 18 in the neural plate and neural plate border and expression at stages 26 and 32 in the branchial arches. Scale bar = 100 μm (Bi) 10x magnification section of a stage 16 embryo showing *CDK9.S* expression in the neural plate and neural plate border (blue) and *Sox10* expression in the neural crest (red). (ii) 20x magnification section shows overlap of the blue *CDK9.S* expression with the red *Sox10* expression. Expression of *CDK9.S* is outlined with a dashed white line and overlaid onto the *Sox10* expression image. Scale bar = 100 μm (C) *CDK9.L* expression at stage 16 and 18 in the neural plate and neural plate border and expression at stages 26 and 32 in the branchial arches. Scale bar = 100 μm (Di) 10x magnification section of a stage 16 embryo showing *CDK9.L* expression in the neural plate and neural plate border (ii) 20x magnification section shows overlap of the blue *CDK9.L* expression with the red *Sox10* expression. Expression of *CDK9.L* is outlined with a dashed white line and overlaid onto the *Sox10* expression image. Scale bar = 100 μm (E) *CyclinT1* expression at stage 15 and 18 in the neural plate and neural plate border and expression at stages 26 and 32 in the branchial arches. Scale bar = 100 μm (Fi) 10x magnification section of a stage 15 embryo showing *CDK9.S* expression in the neural plate and neural plate border (blue) and *Sox10* expression in the neural crest (red). (ii) 20x magnification section shows overlap

of the blue *CDK9.S* expression with the red *Sox10* expression. Expression of *CDK9.S* is outlined with a dashed white line and overlaid onto the *Sox10* expression image. Scale bar = 100 μm. Npb = Neural plate border, ba = branchial arches.

Figure 2: Leflunomide treatment affects the development of neural crest derivatives expression of neural crest genes. (Ai) Top to bottom shows DMSO treated control embryo, 20 μM, 40 μM and 60 μM leflunomide treated *Xenopus laevis* embryos. Leflunomide is applied at stage 15. Scale bar = 500μm (ii) Top to bottom shows DMSO treated control embryo, 60 μM leflunomide applied at stage 1, 8 and 12. Phenotype is observed at stage 38. Black arrow heads indicate pigment cell loss. Scale bar = 300μm (Bi) Graph showing the percentage of embryos displaying a pigment loss phenotype after treatment of DMSO n=155, 20 μM n=158, 40 μM n=164 and 60 μM leflunomide n=141. *=P<0.05 by Kruskall Wallis statistical test. (ii) Graph showing the percentage of embryos displaying a pigment loss phenotype after treatment of DMSO and 60 μM leflunomide applied at stage 1 (DMSO n=60 leflunomide n=72), 8 (DMSO n=67 leflunomide n=73) and 12 (DMSO n=63 leflunomide n=67). *=P<0.05 by Kruskall Wallis statistical test. (C) Whole mount *in situ* hybridisation carried out on embryos treated with either DMSO or 60 μM leflunomide from stage 4 until stage 13 (*Zic1, Zic3* and *Pax3*) or stage 15 (*Sox2*). The neural plate border markers *Zic1, Zic3* and *Pax3* show no change in expression. Similarly, no change is seen for neural plate marker *Sox2*. Scale bar = 200 μm (D) Whole mount *in situ* hybridisation carried out on embryos treated with either DMSO or 60 μM leflunomide from stage 4 until stage 13 (*c*-

Myc) or stage 15 (*Sox10, Slug/Snail2* and *FoxD3*). Specific loss of *c-Myc* expression is seen in the anterior region of the embryo (black arrows) and no loss of expression is seen in the posterior neural tissue. Loss of *Sox10* expression can be seen (black arrows) and some loss or alteration of expression on Slug/*Snail2* and *FoxD3*. Scale bar = 200 μm (E) RNA sequencing carried out on animal caps injected with Wnt-8 and noggin and treated with DMSO or leflunomide. The change in expression seen in specific genes found in the animal cap sample by RNA sequencing is shown. Green = neural crest specifying genes, Orange = neuroectoderm genes, Blue = neural plate border specifiers, Grey = heat shock protein. The complete list of genes affected can be seen in Supplementary data 1.

Figure 3: Knockdown of P-TEFb components leads to loss of expression of neural crest specifying genes. (A) All embryos were injected with 100 ng standard control morpholino, 100 ng CDK9.S morpholino and 60ng CYCLINT1 morpholino in both cells of a two cell stage embryo and fixed at stage 38. Loss of melanocytes in the tail head and lateral stripe are indicated by black arrow heads. (B) All embryos were injected in one cell of a two cell stage embryo with either a control morpholino CoMo, 100 ng CDK9.S morpholino or 60 ng CYCLINT1 morpholino. 300 pg of *Lac-Z* cRNA was co-injected with morpholinos and β-gal activity was detected using a red gal stain to monitor lineage tracing. *in situ* hybridisation was then carried out on these embryos for neural crest specifying, neural plate border and neural plate genes. *c-Myc* (stage 13) shows tissue specific loss of expression (black arrows). *Sox10* (stage 15) shows loss of expression (black arrows). Slug/*Snail2* expression

(stage 15) and *FoxD3* expression (stage 15) appear partially lost or altered. *Zic1* expression (stage 12), *Zic3* expression (stage 12), *Pax3* expression (stage 12) and *Sox2* expression (stage 15) appear unchanged. Quantification of these results can be found in Fig. S5D. Scale bar = 200 μm. (C) Knockdown of P-TEFb components leads to a loss of trigeminal placode markers. All embryos were injected in one cell of a two cell stage embryo with either 100 ng control morpholino (CoMo), 100 ng CDK9.S morpholino or 60 ng CYCLINT1 morpholino. 300 pg of *Lac-Z* cRNA was co-injected with morpholinos and β-gal activity was detected using a red gal stain to monitor lineage tracing. *in situ* hybridisation was then carried out on these embryos for trigeminal placode markers. *Tbx2* expression (stage 18) shows loss of expression specifically in the trigeminal placode region (black arrow). Expression in the otic placode and dorsal root ganglia in not altered. *NeuroD* expression (stage 18) shows specific loss of expression in the trigeminal placode region (black arrow). *ElrD* expression (stage 18) is lost specifically in the trigeminal placode region (black arrow). Expression in the dorsal root ganglia remains unaltered.

Figure 4: c-Myc is a paused gene and CDK9 MO causes c-Myc to become more paused during development.

(A) Histone methylation and RNA polymerase II (RNAPII) binding at the c-Myc gene. Profiles of H3K4me3 (marking active promoters and 5' ends of gene bodies, green), H3K36me3 (showing active transcription, light green) and RNA Pol II (RNAPII, purple) (Hontelez et al., 2015) are visualised using the UCSC Genome Browser for the c-Myc gene on scaffold_6:7,844,903-7,863,621 (*X. tropicalis* genome assembly version 7.1). The transcriptional profile shows *c-*

Myc to be a paused gene in *Xenopus* blastula and gastrula-stage embryos. RNA Pol II profile of the *c-Myc* gene at stage 16 from embryos injected with control MO or Cdk9s MO (blue). Note that the *c-Myc* gene is proportionately more paused in the cdk9 MO treated embryos.

(B) RNA Pol II ChiP-seq on whole embryos injected with Control MO or Cdk9.S MO. i) Histogram plots showing the distribution of the Pausing Index values (RPKM TSS +/- 150bp divided by the RPKM on the gene body) in $\log_2$ space for Control MO-injected (grey) and Cdk9.S MO-injected embryos (orange). The populations were shown to be significantly different from each other (Mann-Whitney P-value<$2.2x10^{-16}$), indicative of RNAPII redistribution. ii) *c-Myc* is more highly paused in Cdk9 MO treated embryos. Scatter plots of RPKM on the gene body versus the transcriptional start site (tss) in Control MO (left panel) and Cdk9.S MO-injected embryos (right panel). The loss of Cdk9 causes an increase in the amount of RNA Pol II bound to the promoter compared to the rest of the gene body. The *c-Myc* gene is shown by the blue spot. Genes with the strongest increase in gene body RNAPII have the lowest increase in PI, suggesting that RNAPII stalls either at the promoter or in the gene body. The effects of RNAPII inhibition on transcript levels is shown in fig 3B.

Figure 5. c-Myc can rescue the effect of Cdk and CyclinT1 morpholino knockdown

(A) Embryos were co-injected into one cell of a two cell stage embryo with a morpholino and *c-Myc* RNA. 300 pg of *Lac-Z* cRNA was co-injected with morpholinos and RNA. β-gal activity was detected using a red gal stain to monitor lineage tracing. Embryos then underwent *Sox10 in situ*. Injection of 100 ng Cdk9.S morpholino and 60 ng CyclinT1 morpholino results in a loss of *Sox10* expression on the injected side. Co-injection of Cdk9.S and CyclinT1 morpholino with 100 pg *c-Myc* RNA results in a partial rescue of *Sox10* expression. Co-injection of Cdk9.S and CyclinT1 morpholino with 500pg *c-Myc* RNA results in a greater rescue of *Sox10* expression. Scale bar = 200 μm. These results are quantified in **Fig. S6D**. (B) Graph showing the percentage of embryos displaying an expansion, wild type, partial loss or loss of *Sox10* expression pattern by *in situ* hybridisation after injection of Cdk9.S morpholino alone (n=51) and co-injected with 100 pg (n=114) and 500 pg of *c-Myc* RNA (n=61). CyclinT1 morpholino alone (n=46) and co-injected with 100 pg (n=61) and 500 pg of *c-Myc* RNA (n=52). 500 pg of *c-Myc* RNA alone (n=34) and 100ng of a standard control morpholino alone (n=33).

Figure 6: Model displaying the mechanism by which *c-Myc* is paused in neural crest cells. On the left *c-Myc* is shown in a paused state with Pol ll bound to NELF, DSIF and Gdown1. We have shown that a knockdown of the P-TEFb components CDK9 and CYCLINT1 leads to a loss of *c-Myc* expression and a subsequent loss of *Sox10* expression and incorrect development of neural crest derivatives (bottom scenario). This suggests in a wild type neural crest cell, P-TEFb is promoting transcriptional elongation of *c-Myc*. P-TEFb in its active form bound to the SEC will phosphorylate DSIF, NELF, Gdown1 and

serine2 of the C terminal of RNA Pol ll. This promotes pause release on the *c-Myc* gene and allows the subsequent expression of *Sox10* leading to correct synchronous development of neural crest derivatives (top scenario). S2 = Serine2, S5 = Serine5, P = phosphorylation mark, NELF = Negative elongation factor, DSIF = DRB sensitivity inducing factor, Pol ll = RNA polymerase II, CDK9 = Cyclin dependent kinase 9, SEC = Super elongation complex.

Figure 1

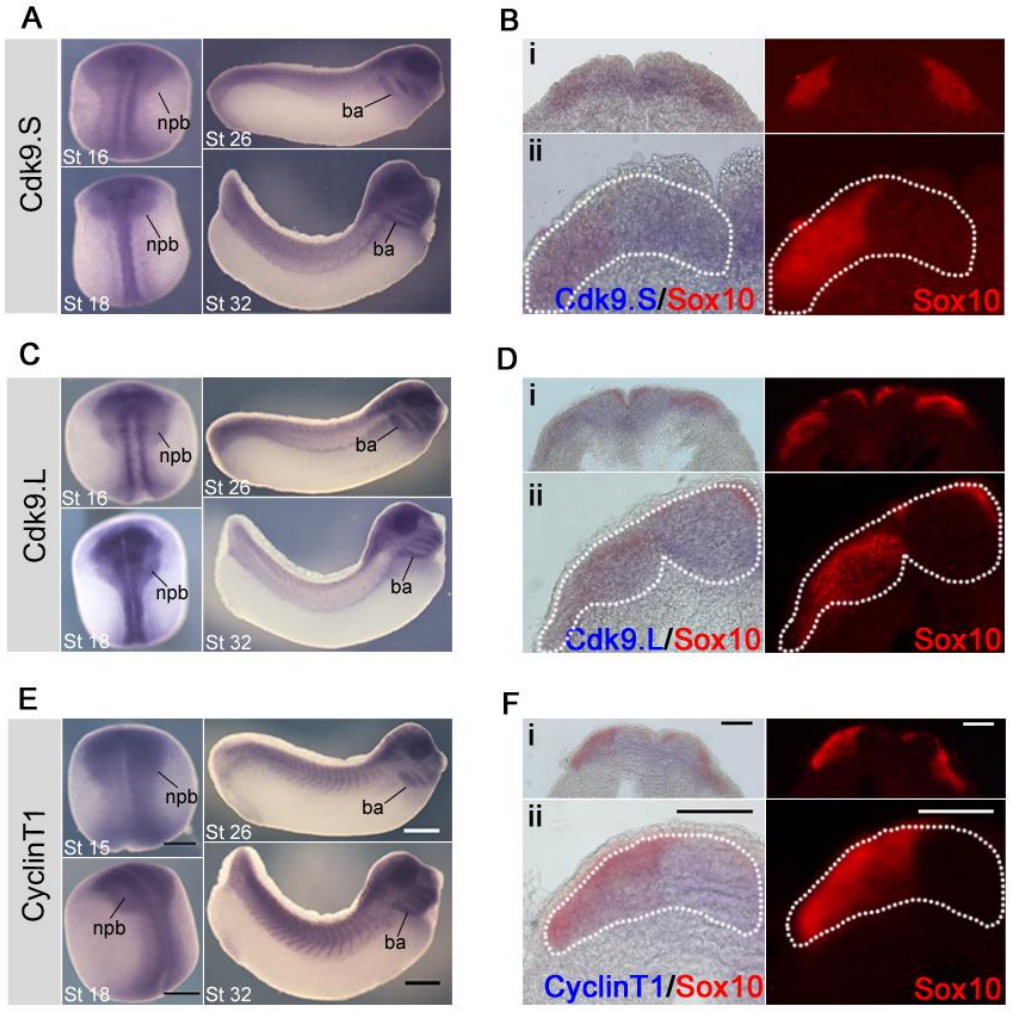
A
Cdk9.S
npb
St 16
ba
St 26
npb
St 18
ba
St 32
B
i
ii
Cdk9.S/Sox10
Sox10
C
Cdk9.L
npb
St 16
ba
St 26
npb
St 18
ba
St 32
D
i
ii
Cdk9.L/Sox10
Sox10
E
CyclinT1
npb
St 15
ba
St 26
npb
St 18
ba
St 32
F
i
ii
CyclinT1/Sox10
Sox10

Figure 2

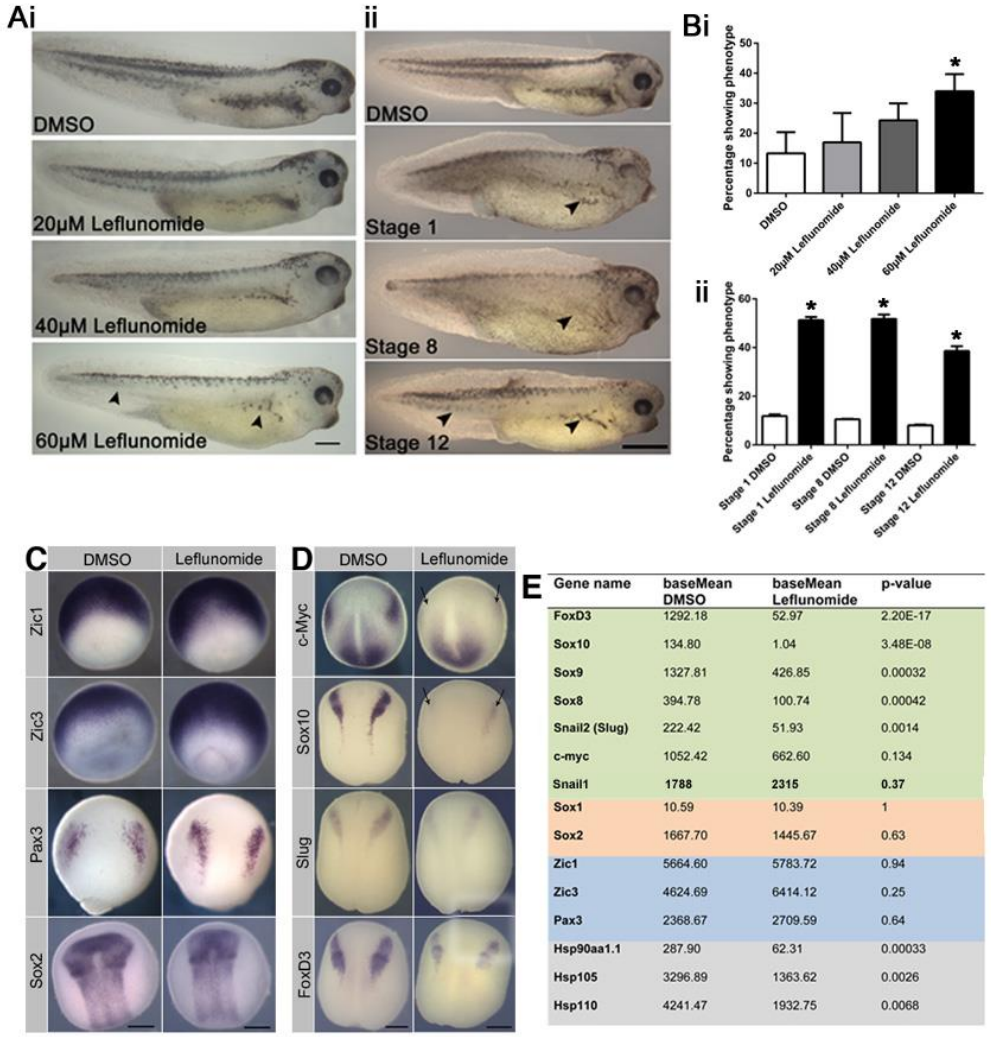

E

Gene name	baseMean DMSO	baseMean Leflunomide	p-value
FoxD3	1292.18	52.97	2.20E-17
Sox10	134.80	1.04	3.48E-08
Sox9	1327.81	426.85	0.00032
Sox8	394.78	100.74	0.00042
Snail2 (Slug)	222.42	51.93	0.0014
c-myc	1052.42	662.60	0.134
Snail1	1788	2315	0.37
Sox1	10.59	10.39	1
Sox2	1667.70	1445.67	0.63
Zic1	5664.60	5783.72	0.94
Zic3	4624.69	6414.12	0.25
Pax3	2368.67	2709.59	0.64
Hsp90aa1.1	287.90	62.31	0.00033
Hsp105	3296.89	1363.62	0.0026
Hsp110	4241.47	1932.75	0.0068

Figure 3

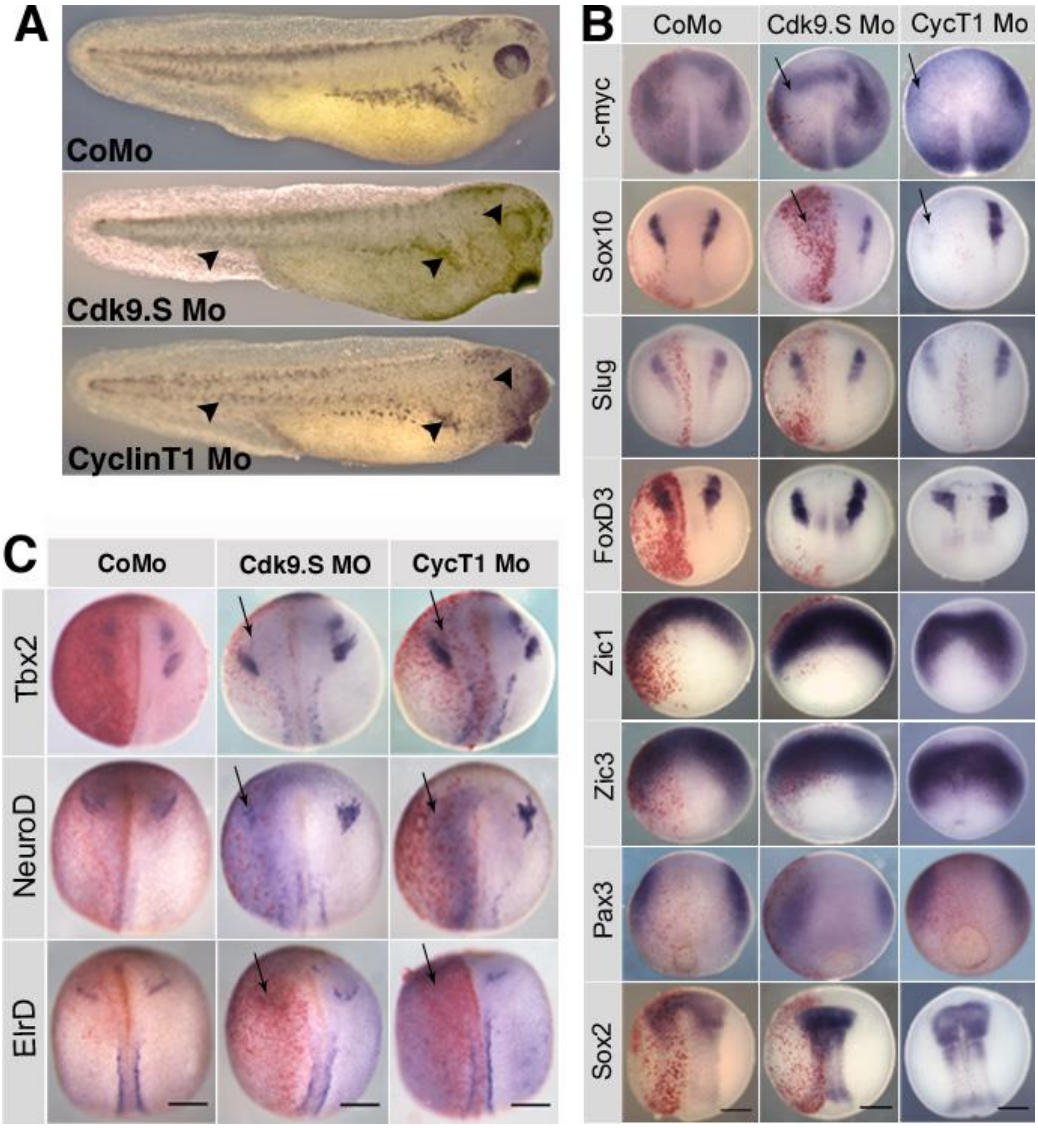
A
CoMo
Cdk9.S Mo
CyclinT1 Mo
B
CoMo
Cdk9.S Mo
CycT1 Mo
c-myc
Sox10
Slug
FoxD3
Zic1
Zic3
Pax3
Sox2
C
CoMo
Cdk9.S MO
CycT1 Mo
Tbx2
NeuroD
ElrD

Figure 4

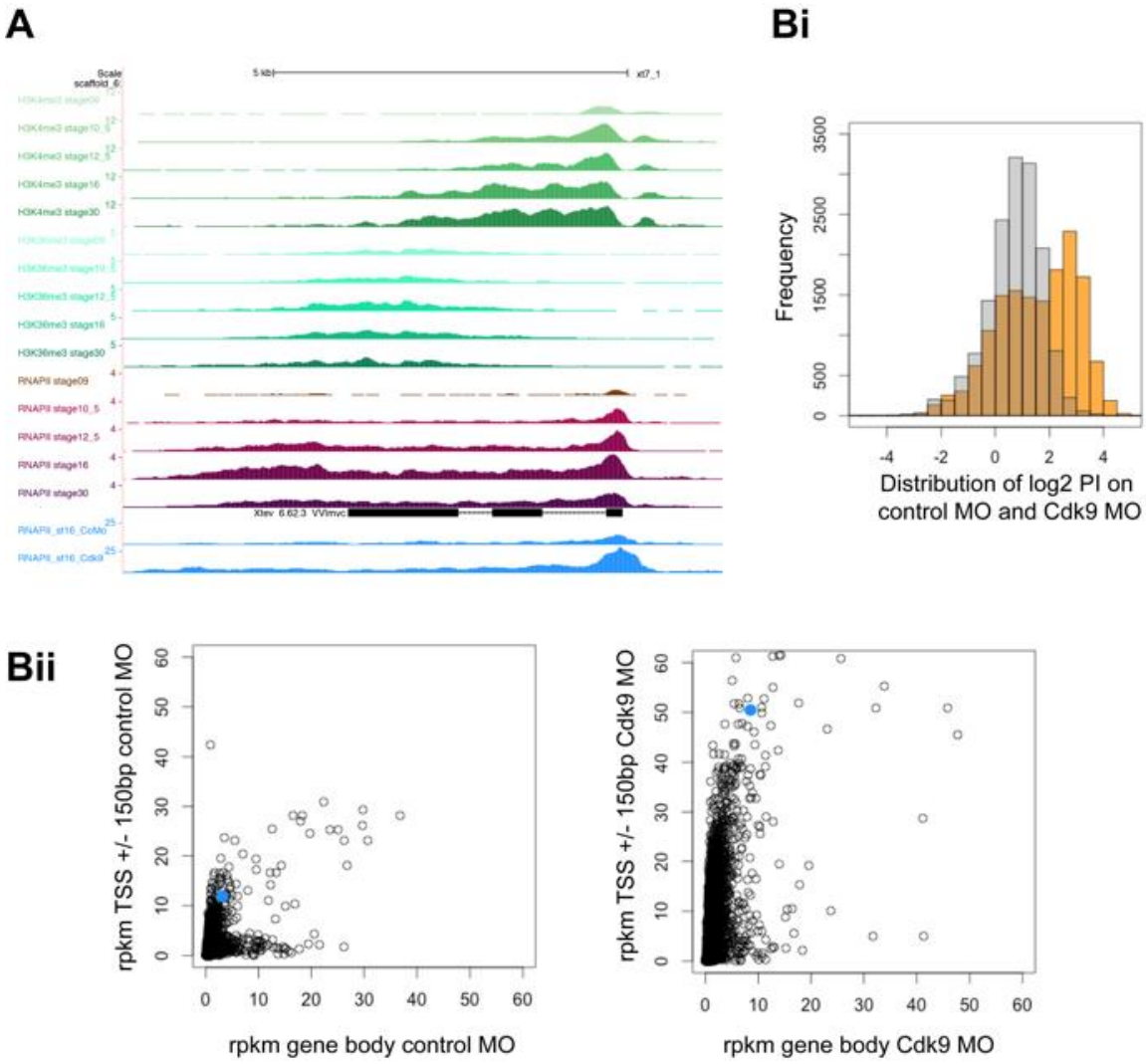
A
Bi
Frequency
Distribution of log2 PI on control MO and Cdk9 MO
Bii
rpkm TSS +/- 150bp control MO
rpkm gene body control MO
rpkm TSS +/- 150bp Cdk9 MO
rpkm gene body Cdk9 MO

Figure 5

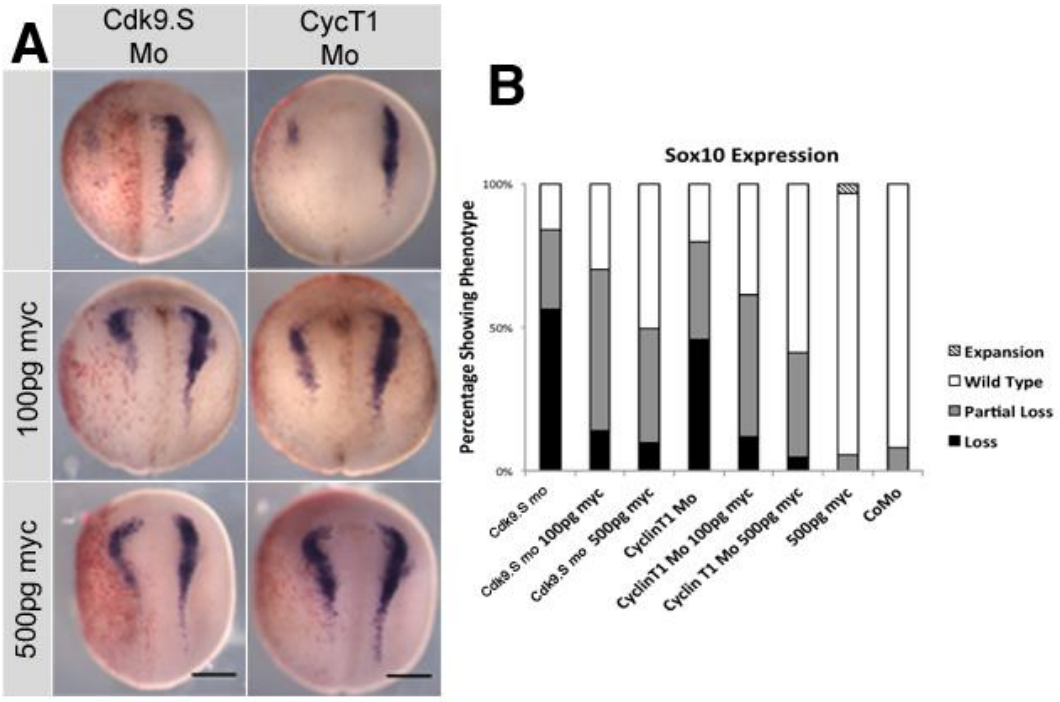
A
Cdk9.S Mo
CycT1 Mo
100pg myc
500pg myc
B
Sox10 Expression
Percentage Showing Phenotype
100%
50%
0%
Cdk9.S mo
Cdk9.S mo 100pg myc
Cdk9.S mo 500pg myc
CyclinT1 Mo
CyclinT1 Mo 100pg myc
Cyclin T1 Mo 500pg myc
500pg myc
CoMo
Expansion
Wild Type
Partial Loss
Loss

Figure 6

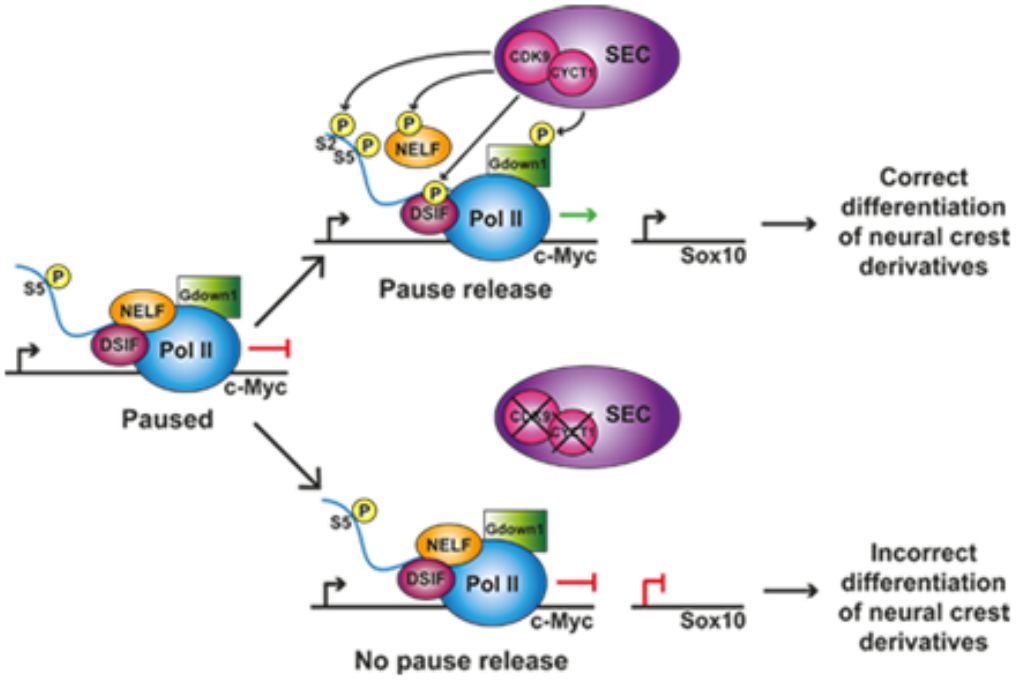
SEC
CDK9
CYCT1
P
S2
S5
NELF
Gdown1
DSIF
Pol II
c-Myc
Pause release
Sox10
Correct differentiation of neural crest derivatives
Paused
No pause release
Incorrect differentiation of neural crest derivatives